Identification and separation of two distinct contributions to the training effect in polycrystalline Co/FeMn bilayers

M. K. Chan,[1] J. S. Parker,[1,2] P. A. Crowell,[1] and C. Leighton[2,*]
[1]*School of Physics and Astronomy, University of Minnesota, Minneapolis, Minnesota 55455, USA*
[2]*Department of Chemical Engineering and Materials Science, University of Minnesota, Minneapolis, Minnesota 55455, USA*
(Received 17 March 2007; revised manuscript received 14 August 2007; published 15 January 2008)

We show that polycrystalline Co/FeMn bilayers display two distinct forms of training effect. The two can be identified and separated via their distinctive field cycle and antiferromagnet thickness dependences, in addition to their influence on the magnetization reversal. One mode is due to the biaxial anisotropy of the antiferromagnet and leads to an abrupt single cycle training (as seen in recent modeling), while the other is a gradual effect related to "depinning" of uncompensated antiferromagnet spins.

DOI: 10.1103/PhysRevB.77.014420 PACS number(s): 75.50.Ee

Fifty years of investigation of exchange bias at antiferromagnet (AF) or ferromagnet (F) interfaces has led to a vastly improved understanding of the effect, although several issues remain unresolved.[1,2] Of the many complex phenomena that accompany the hysteresis loop shift,[1,2] the training effect provides one of the biggest challenges to understanding. Simply stated, the training effect is a decrease in exchange bias (H_E) upon successive field cycling in isothermal hysteresis loop measurements.[1,2] The effect has been observed in a wide variety of materials[1–11] and in some cases[11] is correlated with the existence of magnetization reversal asymmetry (MRA) (i.e., different mechanisms for magnetization reversal on ascending and descending branches of the hysteresis loop).[12–17] In the conventional view training occurs due to a gradual change in the AF spin structure upon repeated field cycling.[1–11] Within the widely accepted model where H_E originates from a finite density of uncompensated AF spins, it can be understood as a thermally activated process leading to gradual depinning of the uncompensated AF spins and a reduction in unidirectional anisotropy.

Recent modeling by Hoffmann[18] provides a new picture for the training effect where the symmetry of the AF's magnetocrystalline anisotropy plays a key role. Using a coherent rotation model, Hoffmann found that biaxial AF anisotropy leads to AF spins freezing into a stable noncollinear configuration which is relaxed after a single field cycle. This results in a single cycle training effect and an accompanying MRA (i.e., sharp reversal on the descending branch and gradual reversal on the ascending branch), similar to that seen in Co/CoO.[11] Recent large-scale micromagnetic simulations on polycrystalline NiFe/NiMn (a biaxial antiferromagnet) bilayers show similar results for an assembly of noninteracting AF grains, even without the implicit assumption of coherent rotation.[19] The simulations suggest that the essence of Hoffmann's model is correct even if the magnetization does not reverse strictly by coherent rotation.

In this paper we show that in biaxial AF/F bilayers (polycrystalline Co/FeMn), both of the above-mentioned mechanisms are active, and that their relative contributions can be deconvolved via their different field cycle and AF thickness dependences as well as by their differing influences on the magnetization reversal mechanisms. The conventional training effect is small, exhibits the well-known $H_E \propto 1/\sqrt{n}$ form (where n is the number of field cycles), and has a weak AF thickness dependence. The contribution due to the biaxial anisotropy of the AF is large, trains out in a single cycle, and is accompanied by a strong MRA. We show that the AF thickness dependence of the latter contribution can be qualitatively understood in terms of Hoffmann's proposed phase diagram.

Polycrystalline Si/a-SiO_2/Cu(300 Å)/Co(60 Å)/$Fe_{1-x}Mn_x$(t_{AF})/Al(30 Å) heterostructures ($0 < t_{AF} < 100$ Å) were grown by UHV dc magnetron sputtering at 300 K in a 300 Oe in-plane field. Growth and structural characterization by x-ray diffraction, x-ray reflectivity, and scanning transmission electron microscopy have been described previously.[20] The $Fe_{1-x}Mn_x$ layers [$x \approx 0.5$ (Ref. 20) hereafter denoted as "FeMn"] have (111) texture and AF/F interface roughness ~8 Å.[20] Broad wide-angle x-ray-diffraction rocking curves are observed (typical full width at half maximum $\geq 5°$) as is typical for metals sputtered at room temperature on Si/a-SiO_2/Cu. Previous experimental and theoretical work demonstrates that bulk FeMn does indeed have biaxial anisotropy.[21,22] Hysteresis loops were measured sequentially using the longitudinal Kerr effect after cooling from 450 K (the measured blocking temperatures of the samples studied here have the same t_{AF} dependence as those in Ref. 20 with the highest blocking temperature of 420 K) to 10 K in a 600 Oe field, applied along the growth field direction. The measurement time (~3 min per loop) was held constant and loops were recorded starting at positive fields with 0.5 Oe field steps within 100 Oe of the switching fields and 3 Oe steps elsewhere. Although the loops are field asymmetric about H_E, they are essentially temporally symmetric (the time spent on the left and right of H_E differ by about 2%).

Figure 1 shows the first, second, third and trained hysteresis loops for t_{AF}=100, 30, and 10 Å measured at 10 K. The trained hysteresis loop is defined as the loop for which $H_E^{n-1} - H_E^n < 0.1$ Oe. Upon field cycling the coercive field on the descending branch decreases faster than the coercive field on the ascending branch. This results in a decrease in H_E with loop number (n) as seen in Fig. 2. The first indication that the training effect is composed of two distinct mechanisms is provided by the observation that a large decrease in H_E occurs between n=1 and n=2 (Figs. 1 and 2), followed by a more gradual decrease for subsequent loops. The con-

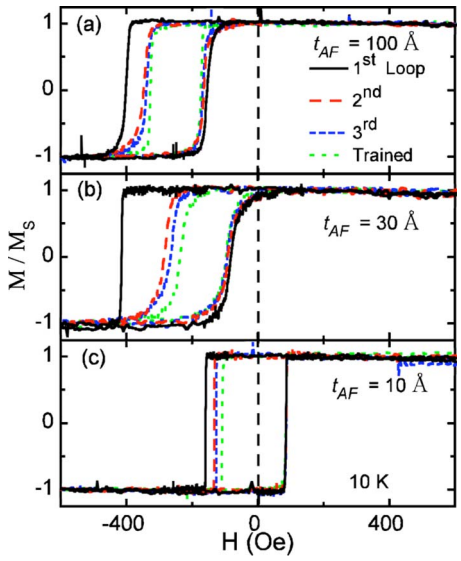

FIG. 1. (Color online) $T=10$ K normalized magnetization hysteresis loops (first, second, third, and last) for $t_{AF}=100$ Å (a), 30 Å (b), and 10 Å (c).

trasting t_{AF} dependences of the first loop and subsequent loop training effects is a second indication. As shown in Fig. 3(a) the first loop training, $H_E^1-H_E^2$, has a strong t_{AF} dependence. It increases by a factor of 5 from 12 Oe at $t_{AF}=10$ Å to 60 Oe at 30 Å, then decreases rapidly, reaching 22 Oe at $t_{AF}=100$ Å. On the other hand, the total training in the subsequent loops $H_E^2-H_E^{20}$ in Fig. 3(b) has weaker t_{AF} dependence, peaking at 20 Å but varying by only a factor of 2 over the whole range. For reference, Fig. 3(b) also shows $H_E^1(t_{AF})$, which increases with increasing t_{AF} before saturating at 40 Å. The exact relationship between $H_E^1(t_{AF})$, $H_E^1-H_E^2(t_{AF})$, and $H_E^2-H_E^{20}(t_{AF})$ will be discussed later. As a check, field symmetric loops with measurement time per loop approximately 5 times longer were repeated on one sample ($t_{AF}=30$ Å) and show negligible difference in total training ($\sim$5% increase) and no change in the results discussed below.

A further indication that two distinct training mechanisms are active is that the first loop training effect is also accompanied by MRA. As shown in Fig. 1(b) the descending branch of the $n=1$ loop has an abrupt reversal while the

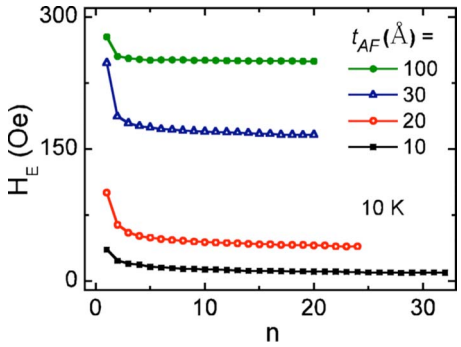

FIG. 2. (Color online) $T=10$ K exchange bias H_E as a function of loop number n for $t_{AF}=100$, 30, 20, and 10 Å.

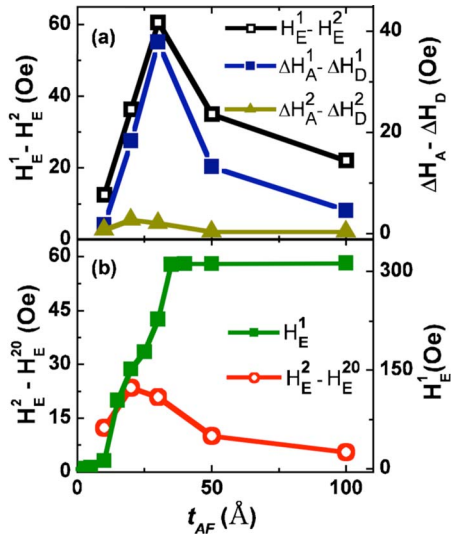

FIG. 3. (Color online) T=10K (a) First cycle training ($H_E^1-H_E^2$), and difference in switching widths between ascending and descending branches ($\Delta H_D-\Delta H_A$) (right axis) for the first and second loops as a function of AF thickness. (b) Subsequent training ($H_E^2-H_E^{20}$) and initial exchange bias H_E^1 as a function of AF thickness.

ascending branch reverses gradually. This is only evident for $n=1$ and does not occur during the gradual subsequent training, i.e., $n\geq 2$. Additional evidence for this is provided by transverse (Fig. 4) and minor (Fig. 5) loop measurements. Figure 4 shows transverse loop measurements performed using a SQUID magnetometer with a "vector" coil set. The $n=1$ (virgin) loop [Fig. 4(a)] has a small transverse moment on the descending branch (which peaks at the coercive field), but a larger moment on the ascending branch. This MRA is not present on the trained loop [Fig. 4(b)] where the transverse magnetization is approximately equal on each side of the loop. Figure 5 shows descending and ascending branch minor loops performed on a $t_{AF}=20$ Å sample. In Fig. 5(a) the sample was first field cooled to 40 K from above the

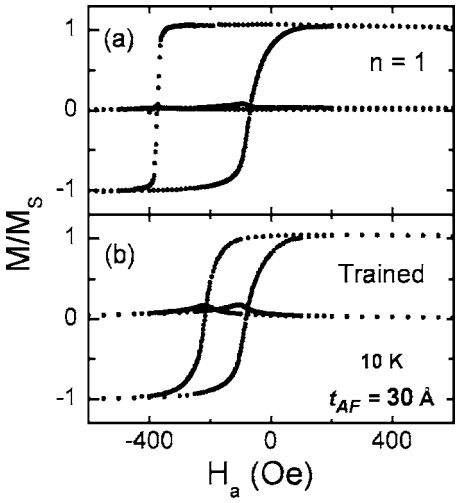

FIG. 4. Longitudinal and transverse hysteresis loops for $t_{AF}=30$ Å at $T=10$ K. (a) $n=1$ (virgin) loop. (b) Trained loop.

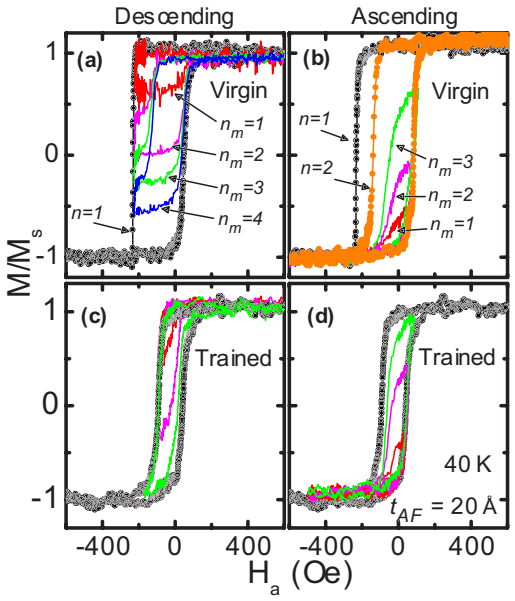

FIG. 5. (Color online) Minor loops for $t_{AF}=20$ Å at $T=40$ K. (a) Minor loops for the virgin descending branch $n_m=1$, 2, 3, and 4 (red, magenta, green, and blue lines) and the full $n=1$ (virgin) loop (black circles). (b) Minor loops for the virgin ascending branch $n_m=1$, 2, and 3 (red, magenta, and green lines). The $n=1$ (virgin) descending branch (black circles) and $n=2$ loop (orange circles) are also shown. (c) Minor loops for the trained descending branch and a trained loop. (d) Minor loops for the trained ascending branch and a trained loop.

blocking temperature. The first minor hysteresis loop ($n_m=1$, where n_m is the minor loop number upon field cooling) was then obtained by interrupting the first field sweep on the descending branch [the red line in Fig. 5(a)] and then returning to the maximum positive field. Loops $n_m=2$, 3, and 4 [magenta, green, and blue lines in Fig. 5(a)], were then measured, each by interrupting the field sweep successively further down the descending branch than the prior minor loop. The sample was then warmed above T_B and field cooled to 40 K again, where full $n=1$ and $n=2$ loops were measured for reference. The same process was repeated to obtain $n_m=1$, 2, and 3 loops on the ascending branch [Fig. 5(b)]. We observe that the descending branch minor loops have essentially the same maximum width as the $n=1$ loop, while the ascending branch minor loops are significantly narrower than the $n=2$ loop. As will be discussed below, these observations indicate different switching mechanisms on either side of the $n=1$ loop. Corresponding minor loops for the trained case show that the MRA vanishes for $n>1$ [Figs. 5(c) and 5(d)].

A measure of MRA is the difference between the ascending and descending branch switching widths ($\Delta H_D-\Delta H_A$) defined as the field range between $0.8M_S$ and $-0.8M_S$. As seen in Fig. 3(a), the MRA for the first loop ($\Delta H_D^1-\Delta H_A^1$) has the exact same t_{AF} dependence as $H_E^1-H_E^2$ while the second loop MRA ($\Delta H_D^2-\Delta H_A^2$) is significantly reduced. This indicates that the same mechanism is responsible for both the first loop MRA and the first cycle training and that this mechanism is not active on subsequent loops. In summary, the distinct difference in the character of $H_E(n)$ for $n=1$ and $n\geq 2$, the existence of MRA only for $n=1$, and the differing AF thickness dependence of $H_E^1-H_E^2$ and $H_E^2-H_E^{20}$ are all clear indications that two training mechanisms are active in this system.

Recent modeling of biaxial AF/F systems by Hoffmann has revealed a large single cycle training effect accompanied by strong MRA.[18] In Hoffman's model, frustration between the coupling of the two AF sublattices and the interfacial coupling between the AF and F leads to a state where the AF sublattices align perpendicularly. When the F magnetization is reversed the AF sublattices realign into an antiparallel configuration and this configuration is maintained for subsequent loops, leading to a single cycle training effect. The F magnetization is therefore found to switch abruptly on the first descending branch and more gradually on all subsequent branches. We believe that the Hoffmann model provides a good description of our data on this biaxial AF/F system (FeMn/Co), being responsible for the $n=1$ training component. Additionally, the observation that all of the minor loops on the virgin descending branch have essentially the same maximum width as the full $n=1$ loop [Fig. 5(a)] indicates that the initial magnetization reversal is domain driven and completely irreversible, consistent with the realignment of AF sublattices proposed by Hoffmann. In contrast, minor loops obtained on the ascending branch of the first loop [Fig. 5(b)] have much smaller widths; even a minor loop with 80% of a full loop's height has only approximately half the width [Fig. 5(b)]. Minor loops obtained on fully trained loops [Figs. 5(c) and 5(d)] are also significantly narrower than the full loop. It is therefore clear that a large reversible component is present in these subsequent reversals. It should be noted that Hoffmann's work utilized a coherent rotation model, which would predict a transverse moment magnitude of approximately M_S on the $n=1$ ascending branch.[18] We observe, however, a much smaller transverse moment [Fig. 4(a)]. One of the reasons for this, as is evident from the minor loops in Fig. 5(b), is that the reversal mechanism on the ascending branch is a mixture of rotation and domain processes. Furthermore, the rotation of the magnetization is not necessarily uniform from grain to grain. The "granular" nature of the reversal process can be seen most clearly in Fig. 5(a). The $n_m=2$ descending branch consists of two parts. The first part, characterized by a smaller coercivity and gradual reversal, extends to the point where the $n_m=1$ field sweep was interrupted. It therefore involves grains that have already been trained by the Hoffmann mechanism. The second part, which has the full width of a virgin loop and sharp reversal, involves grains that were not accessed during the $n_m=1$ loop and were therefore not trained. In this manner, the fraction of grains that are trained by the Hoffmann mechanism increases with each successive minor loop.

The t_{AF} dependence of the first cycle training ($H_E^1-H_E^2$) and the MRA is also qualitatively consistent with this model. According to Hoffmann, for large t_{AF} the antiferromagnetic coupling between sublattices dominates over the AF/F interface coupling, leading to antiparallel alignment of the sublattices when field cooled. On the other hand, for sufficiently small t_{AF}, coupling to the F dominates and both AF sublattices align parallel to the F magnetization. Both of these situations result in no training or MRA. The t_{AF} dependence

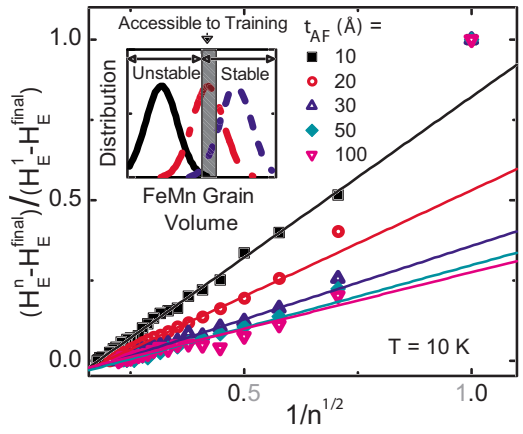

FIG. 6. (Color online) Normalized residual training $(H_E^n - H_E^{final})/(H_E^1 - H_E^{final})$ vs $1/\sqrt{n}$ for t_{AF}=100, 50, 30, 20, and 10 Å. The solid lines are straight line fits for $n \geq 3$. Inset: Schematic illustration of the grain size distributions at t_{AF}=10, 20, and 40 Å (from left to right). The region of thermal stability at 10 K is labeled. The shaded area marks the region that becomes thermally unstable upon alignment of the F magnetization antiparallel to the cooling field.

of $H_E^1 - H_E^2$ [Fig. 2(b)], and the MRA (Fig. 1) are therefore in qualitative agreement with the model. Clearly the decrease in $H_E^1 - H_E^2$ for $t_{AF} < 40$ Å is also related to the decrease in H_E^1.

According to the Hoffmann model the training effect should disappear for $n \geq 2$, in contrast to our data (Fig. 2). As discussed above, a second training mechanism is therefore active, which we believe has its origin in conventional thermal "depinning" of uncompensated AF spins. Conventional multiloop training has been observed previously in many F/AF systems and has been shown to follow an empirical $H_E \propto 1/\sqrt{n}$ dependence.[1,3,6] This is generally attributed to reorientation of uncompensated AF spins during magnetization reversal due to thermal activation.[1–10] In Fig. 6 the quantity $(H_E^n - H_E^{final})/(H_E^1 - H_E^{final})$ (i.e., the residual training normalized to the total extent of training) is plotted as a function of $1/\sqrt{n}$. The $1/\sqrt{n}$ form is adhered to very well for $n > 2$ (when conventional training is active), but fails completely at $n=1$ (Hoffmann training), a graphic illustration of the existence of two components.

The t_{AF} dependence of this second contribution to the training can be qualitatively understood in terms of thermal stability of the AF grains, which are the source of uncompensated spins that give rise to H_E. At this stage we make the assumption that each AF grain acts as a single domain. This is supported by a simple calculation, which suggests that the domain wall width in the AF is ~3 nm, comparable to the grain size from TEM (5–10 nm). Note that this calculation uses an AF anisotropy of 6×10^6 erg/cm^3 (Ref. 23) while recent work[24] suggests that values distributed between zero and 6×10^6 erg/cm^3 are required to model the data on this system. 3 nm should therefore be taken as a lower limit for the domain wall width, further strengthening our assumption of single domain behavior for the AF grains. As is well understood, the behavior of $H_E^1(t_{AF})$ [Fig. 2(b)] can be simply explained in terms of thermal stability of the assembly of grains comprising the polycrystalline AF pinning layer.[1,2,25] Thermal fluctuations in the AF layer occur at a rate proportional to $\exp\{-\delta E/k_B T\} = \exp\{-K_{AF} V_{AF}(1 \pm H^*/H_K)/k_B T\}$, where V_{AF} is the volume of the AF grain, K_{AF} is the AF anisotropy constant, H^* is the effective field experienced by the AF grains (which has a large component due to exchange coupling with the adjacent F, and can therefore be switched with the F magnetization), and H_K is the AF anisotropy field. We assume a distribution in AF grain volumes,[23] with an average grain volume that increases with t_{AF}. The data of Fig. 3(b) (T=10 K) show that the AF grains are essentially all thermally stable (over the time scale of the experiment) at t_{AF}=40 Å, and unstable at t_{AF}=10 Å. In the intermediate region (10 Å $< t_{AF} <$ 40 Å) the fraction of grains that is thermally stable increases with t_{AF}. These three cases are represented by the three grain volume distributions shown schematically in the inset to Fig. 6. We assign $t_{AF} \approx 10$, 20, and 40 Å to these distributions based on the observed $H_E^1(t_{AF})$ shown in Fig. 3(b). When the F magnetization is aligned opposite to the cooling field during measurement of the hysteresis loop the energy barrier is reduced to $\delta E = K_{AF} V_{AF}(1 - H^*/H_K)$ and a fraction of the AF grains now become unstable (as shown by the shaded region in the inset to Fig. 6) leading to a reduction in bias and therefore a training effect. The amount of training at a given t_{AF} is simply related to the extent of overlap between this shaded region and the grain size distribution, which clearly therefore peaks near 20 Å, i.e., midway between the AF thickness at which nonzero bias is first observed and that at which the bias saturates [see Fig. 3(b)]. Although the above argument is cast in terms of a distribution in grain sizes, similar arguments will hold for any situation where there exists a distribution in energy barriers to reversal, e.g., a model where individual uncompensated spins in the AF are gradually depinned by successive magnetization reversals in the F.

In summary, we observe two distinct contributions to the training effect in polycrystalline biaxial AF/F bilayers. The first component is large, trains out in a single cycle, has a strong AF thickness dependence, and has accompanying magnetization reversal asymmetry. We associate this contribution with the existence of a biaxial AF anisotropy. The second component is smaller, has a more gradual loop number dependence, a weaker thickness dependence, and no accompanying reversal asymmetry. We interpret this contribution as being due to a conventional mechanism due to thermally activated depinning. The AF thickness dependence of both contributions can be qualitatively understood in terms of simple models.

We would like to thank J. Saha and R. Victora for illuminating discussions. This work was supported by the NSF MRSEC program and NSF Grant No. DMR 04-06029.

*Corresponding author; leighton@umn.edu

[1] J. Nogués and I. K. Schuller, J. Magn. Magn. Mater. **192**, 203 (1999).
[2] A. E. Berkowitz and K. Takano, J. Magn. Magn. Mater. **200**, 552 (1999).
[3] D. Paccard, C. Schlenker, O. Massenet, R. Montmory, and A. Yelon, Phys. Status Solidi **16**, 301 (1966).
[4] C. H. Lai, H. Matsuyama, R. L. White, T. C. Anthony, and G. G. Bush, J. Appl. Phys. **79**, 6389 (1996).
[5] H. Xi, R. M. White, S. Mao, Z. Gao, Z. Yang, and E. Murdock, Phys. Rev. B **64**, 184416 (2001).
[6] A. Hochstrat, C. Binek, and W. Kleemann, Phys. Rev. B **66**, 092409 (2002).
[7] J. Keller, P. Miltényi, B. Beschoten, G. Güntherodt, U. Nowak, and K. D. Usadel, Phys. Rev. B **66**, 014431 (2002).
[8] H. Y. Li, L. Y. Chen, and S. M. Zhou, J. Appl. Phys. **91**, 2243 (2002).
[9] J. Dho, C. W. Leung, and M. G. Blamire, J. Appl. Phys. **99**, 033910 (2006).
[10] L. E. Fernandez-Outon, G. Vallejo-Fernandez, S. Manzoor, and K. O'Grady, J. Magn. Magn. Mater. **303**, 296 (2006).
[11] S. G. E. teVelthuis, A. Berger, G. P. Felcher, B. K. Hill, and E. D. Dahlberg, J. Appl. Phys. **87**, 5046 (2000); W. T. Lee, S. G. E. teVelthuis, G. P. Felcher, F. Klose, T. Gredig, and E. D. Dahlberg, Phys. Rev. B **65**, 224417 (2002).
[12] V. I. Nikitenko, V. S. Gornakov, A. J. Shapiro, R. D. Shull, K. Liu, S. M. Zhou, and C. L. Chien, Phys. Rev. Lett. **84**, 765 (2000).
[13] M. R. Fitzsimmons, P. Yashar, C. Leighton, I. K. Schuller, J. Nogués, C. F. Majkrzak, and J. A. Dura, Phys. Rev. Lett. **84**, 3986 (2000); C. Leighton, M. R. Fitzsimmons, P. C. Yashar, A. Hoffmann, J. Nogués, J. A. Dura, C. F. Majkrzak, and I. K. Schuller, *ibid.* **86**, 4394 (2001).
[14] H. D. Chopra, D. X. Yang, P. J. Chen, H. J. Brown, L. J. Swatzendruber, and W. F. Egelhoff, Jr., Phys. Rev. B **61**, 15312 (2000).
[15] T. Mewes, H. Nembach, M. Rickart, S. O. Demokritov, J. Fassbender, and B. Hillebrands, Phys. Rev. B **65**, 224423 (2002); T. Mewes, H. Nembach, J. Fassbender, B. Hillebrands, J. V. Kim, and R. L. Stamps, *ibid.* **67**, 104422 (2003).
[16] X. Portier, A. K. Petford-Long, A. de Morais, N. W. Owen, H. Laidler, and K. O'Grady, J. Appl. Phys. **87**, 6412 (2000).
[17] J. Camarero, J. Sort, A. Hoffmann, J. M. García-Martín, B. Dieny, R. Miranda, and J. Nogués, Phys. Rev. Lett. **95**, 057204 (2005).
[18] A. Hoffmann, Phys. Rev. Lett. **93**, 097203 (2004).
[19] J. Saha and R. H. Victora, Phys. Rev. B **73**, 104433 (2006).
[20] B. Bolon, M. A. Haugen, A. Abin-Fuentes, J. Deneen, C. B. Carter, and C. Leighton, J. Magn. Magn. Mater. **309**, 1 (2006).
[21] H. Umebayashi and Y. Ishikawa, J. Phys. Soc. Jpn. **21**, 1281 (1966).
[22] J. M. MacLaren, S. Crampin, and D. D. Vvedensky, Phys. Rev. B **40**, 12176 (1989).
[23] K. Nishioka, C. Hou, H. Fujiwara, and R. D. Metzger, J. Appl. Phys. **80**, 4528 (1996).
[24] J. Saha, J. S. Parker, B. Bolon, A. Abin-Fuentese, C. Leighton, and R. H. Victora, J. Appl. Phys. **102**, 073901 (2007).
[25] S. Manzoor, M. Vopsaroiu, G. Vallejo-Fernandez, and K. O'Grady, J. Appl. Phys. **97**, 10K118 (2005).